CORROSION SCIENCE AND TECHNOLOGY, Vol.24, No.3(2025), pp.162~174 pISSN 1598-6462 / eISSN 2288-6524
[Research Paper] DOI: https://doi.org/10.14773/cst.2025.24.3.162

Investigating SDS Surfactant as a Corrosion Inhibitor for Carbon Steel in Hydrochloric Acid: Mechanisms and Efficacy

Duhak Ahmed Alwan and Oraas Adnan Hatem†

Department of Chemistry, College of Science, University of AL-Qadisiyah, Iraq
(Received August 12, 2024; Revised August 26, 2024; Accepted January 30, 2025)

The corrosion inhibition performance of sodium dodecyl sulfate (SDS) for carbon steel (CS) in 1 M hydrochloric acid (HCl) environments was rigorously evaluated using potentiodynamic polarization techniques. This study explored efficacies of SDS at various concentrations and temperatures (20, 30, 40, and 50 °C) for inhibiting corrosion of CS. Findings demonstrated a notable anti-corrosion effect of SDS, with the maximum inhibition efficiency reaching 70% at 20 °C. The adsorption behavior of SDS conformed to the Langmuir adsorption isotherm as indicated by high correlation coefficients. Computed standard adsorption free energy values suggested that both physisorption and chemisorption of SDS occurred on the CS surface. Surface analyses, including atomic force microscopy (AFM) and scanning electron microscopy (SEM), revealed the formation of a uniform protective layer, evidenced by smoother AFM images and reduced corrosion damage in SEM micrographs. A computational investigation using the PM3 method offered additional insights into the observed inhibition efficiencies, enhancing comprehension of the mechanism of action of SDS invovled in inhibiting corrosion of CS.

Keywords: *Corrosion inhibitor, SDS, Carbon steel, Isotherms, Potentiodynamic polarization*

1. Introduction

Acidic solutions are commonly employed in industrial applications such as steel pickling, chemical refining, and oil well acidification, but these processes often result in significant corrosion of carbon steel components like machinery, tubes, and pipelines [1]. Corrosion presents both economic and safety challenges, prompting extensive research into understanding and mitigating its effects, particularly in acidic environments [2].

Carbon steel is frequently used as a model material to investigate corrosion prevention in acidic conditions. Chemical inhibitors, including ammonium salts, heterocyclic compounds, Schiff bases, and amino acids [3-5], are typically utilized to reduce the corrosion rate by forming protective layers on the metal surface through chemisorption or physisorption [6].

Surfactants have gained attention as effective corrosion inhibitors due to their strong adsorption onto metal surfaces, which enhances the formation of protective layers and improves corrosion resistance [7]. Research has shown that surfactants can significantly boost the adsorption of inhibitory agents, making them a valuable focus for corrosion protection studies [8].

The objective of this article is to investigate the use of sodium dodecyl sulfate (SDS) as a surfactant-based corrosion inhibitor for carbon steel in hydrochloric acid environments. The study aims to elucidate the mechanisms by which SDS inhibits corrosion, evaluate its efficacy compared to other inhibitors, and explore its potential for improving the protection of carbon steel in industrial applications where acidic conditions prevail.

2. Experimental Methods

2.1 Material

Sodium dodecyl sulfate (SDS) and hydrochloric acid (HCl) were obtained from Sigma-Aldrich and used as received. Carbon steel pipelines (dimensions 2 × 2 × 0.3 cm, composition detailed in Table 1) were hand-polished sequentially with emery papers of grades 180, 600, 800, and finally 1200. Before each experiment, the metal surfaces were cleaned with acetone, benzene, and deionized water.

†Corresponding author: oraas.adnan@qu.edu.iq

Table 1. Carbon steel Chemical compositions

Fe%	C%	Mn%	P%	Si%	S%	Al%
balance	0.28	1.24	0.03	0.35	0.04	0.02

2.2 Method

Electrochemical experiments were performed with a CH Instrument 660E potentiostat/galvanostat. All corrosion tests utilized a three-electrode setup, consisting of Carbon steel as the working electrode, a Pt wire as the counter electrode, and an Ag/AgCl electrode as the reference. PDP measurements were conducted with a scan rate of 0.01 V/s. The polarization curves for carbon steel, both with and without different inhibitor concentrations, were recorded over a range from -0.8 to -0.1 V.

The inhibition efficiency (IE%) was calculated based on the corrosion current density using the following formula: [9].

$$IE\% = \left(\frac{i^{o}_{corr} - i_{corr}}{i^{o}_{corr}}\right) \times 100 \quad (1)$$

Here, i^{o}_{corr} represents the corrosion current density without the inhibitor, and i_{corr} is the corrosion current density with the inhibitor present.

2.3 Quantum chemical calculations

The adsorption behavior of SDS surfactant on the surface of carbon steel was investigated through the analysis of quantum chemical parameters. The molecular structure of SDS was optimized using the Chem Draw 3D simulation tool. Key quantum chemical parameters, such as the energy gap between the lowest unoccupied molecular orbital (LUMO) and the highest occupied molecular orbital (HOMO) (ΔE), dipole moment (μ), energy of the LUMO (ELUMO), and energy of the HOMO (EHOMO), were determined to assess the interaction of SDS with the steel surface. Additionally, the ionization potential (IP) and electron affinity (A), which are intrinsically linked to the energies of HOMO and LUMO, were calculated according to equations (2) and (3).

$$IP = -E_{HOMO} \quad (2)$$

$$A = -E_{LUMO} \quad (3)$$

Absolute electronegativity (χ) of the inhibitor is given by

$$\chi = -\frac{1}{2}(E_{HOMO} + E_{LUMO}) \quad (4)$$

andabsolutehardness (η)

$$\eta = \frac{E_{LUMO} - E_{HOMO}}{2} \quad (5)$$

Adsorption is most likely to occur at the molecular fragment where the softness (ζ) is maximized, calculated as $\zeta = 1/2\eta$, allowing for the most efficient electron transfer. Parr introduced the global electrophilicity index (ω), which helps in evaluating a species' ability to accept electrons, also known as electron affinity. Lower values of the chemical potential (μ) and electrophilicity index (ω) indicate a more reactive nucleophile, while higher values suggest a stronger electrophile. The electrophilicity index is defined by $\omega = \frac{\mu^2}{2\eta}$. The number of electrons transferred (ΔN) between the inhibitor and iron can be calculated using the formula

$$\Delta N = \frac{X_{Fe} - X_{inh}}{2(\eta_{Fe} + \eta_{inh})} \quad (6)$$

where X_{inh} and X_{Fe} represent the absolute electronegativities of the inhibitor and iron, respectively, and η_{inh} and η_{Fe} represent the absolute hardness of the inhibitor and iron, respectively [10-12].

2.4 Surface analysis

The surface morphology and topography of corroded carbon steel samples were evaluated both with and without the presence of inhibitors. Initially, the polished carbon steel specimens were examined using an optical microscope to analyze the surface morphology before any corrosion reactions began. This preliminary examination was conducted to detect and exclude specimens with surface defects, such as pits, cracks, or other visible irregularities. Only specimens with a smooth, defect-free surface were selected for immersion under the designated conditions. After the corrosion tests were completed, the specimens were carefully rinsed with double-distilled water, dried, and then analyzed using scanning electron microscopy (SEM) and atomic force microscopy (AFM) to evaluate their surface morphology and topography.

3. Results

3.1 Electrochemical study

Table 2, Fig. 1, Fig. 2.

3.2. Thermodynamic and activation parameters study

Fig. 3, Table 3.

3.3 Adsorption isotherms

Fig. 4.

3.4 Surface morphological study

3.4.1 Field Emission -Scanning Electron Microscopy FE-SEM

Fig. 5.

3.4.2 Field Atomic Force Microscopy AFM

Fig. 6

3.5 Quantum chemical study

Table 5, Fig. 7.

4. Discussion

4.1 Electrochemical study

Potentiodynamic polarization measurements provide crucial insights into the kinetics of both anodic and cathodic corrosion reactions [13]. Key electrochemical corrosion parameters include the corrosion potential (E_{corr}), corrosion current density (I_{corr}), along with the anodic and cathodicTafel constants (β_a and β_b), and the

Table 2. Potentiodynamic polarizationparameters of carbon steel in acidic medium at various concentrations of SDS and temperatures

Con.(M) of SDS	T (°C)	i_{corr} (mA/cm^2)	E_{corr} (V)	β_a	β_c	EI (%)
In the absence of an inhibitor	20	5.349	- 0.4382	7.609	7.506	-----
	30	9.378	-0.4408	6.507	6.749	-----
	40	23.75	-0.4432	5.19	5.294	-----
	50	25.05	-0.4348	5.824	4.906	-----
1×10^{-4}	20	3.747	-0.4167	8.853	5.974	29.9
	30	6.738	-0.4244	7.009	5.475	28.1
	40	17.93	-0.4224	6.119	5.342	24
	50	20.2	-0.4234	6.165	4.806	19
8×10^{-4}	20	3.577	-0.4331	7.601	7.165	33
	30	6.608	-0.4194	7.326	4.978	29.5
	40	17.54	-0.4279	6.516	5.145	26.1
	50	21.33	-0.4150	6.588	4.698	14.8
1×10^{-3}	20	2.351	-0.4236	9.188	6.912	56
	30	5.131	-0.4313	8.903	5.926	45.2
	40	13.15	-0.4222	6.468	5.176	44.6
	50	15.4	-0.4122	6.347	5.034	38.5
8×10^{-3}	20	2.269	-0.4339	7.168	6.481	58.3
	30	4.596	-0.4337	6.517	6.245	50.9
	40	12.17	-0.4312	5.996	4.518	48.7
	50	14.64	-0.4227	5.959	4.694	41.6
4×10^{-2}	20	1.600	-0.4330	7.721	7.585	70
	30	3.218	-0.4050	9.665	6.14	65.6
	40	11.05	-0.4279	5.854	5.219	53.4
	50	13.17	-0.4278	5.489	5.098	47.4

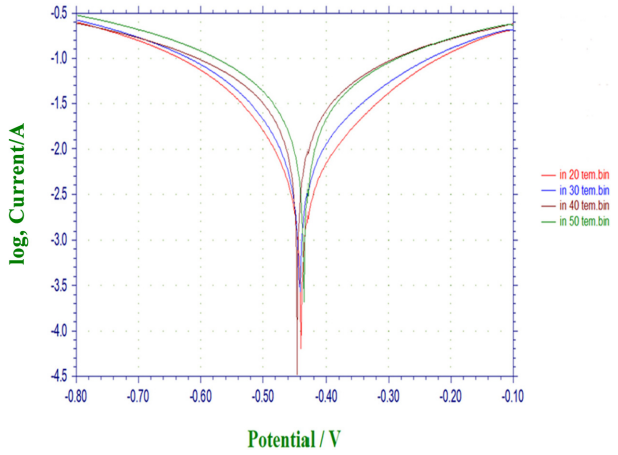

Fig. 1. Potentiodynamic polarization curves for Carbon steel in 1M HCL in the absence of inhibtor at 20-50 °C

corrosion inhibition efficiency (%). These parameters were determined from Potentiodynamic polarization curves (E–log I) for carbon steel submerged in hydrochloric acid (HCl) solutions, both without and with the addition of SDS surfactant. The corresponding values are presented in Table 2.

The potentiodynamic polarization analysis was conducted to evaluate the inhibitory effects of SDS surfactant at varying concentrations (M) and different temperatures on corrosion in 1.0 M HCl. The results from the potentiodynamic tests, along with the variations in open circuit potential (E_{ocp}), are illustrated in (Fig.s 1 and 2.).

The current and the corresponding charge under the

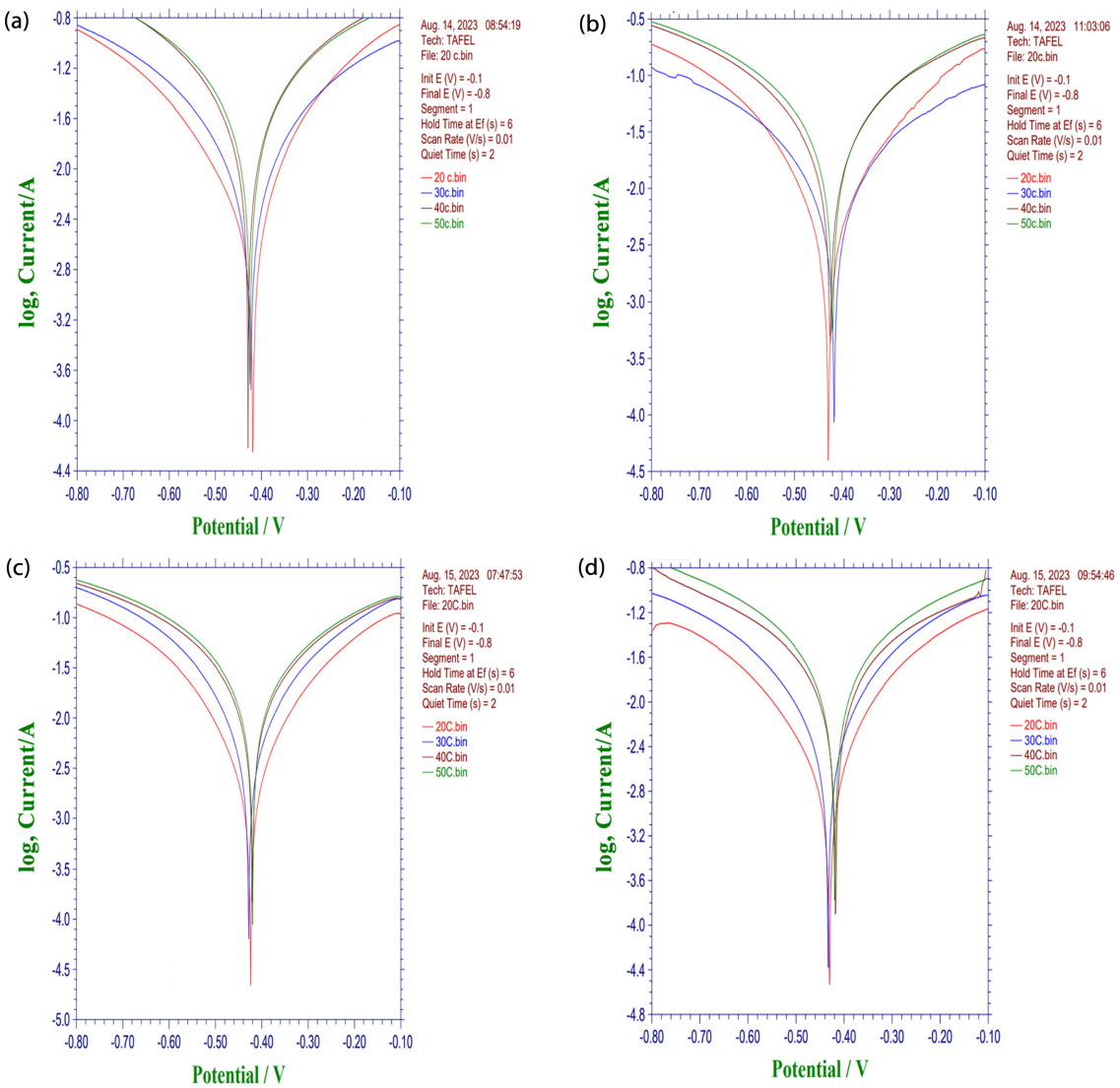

Fig. 2. Potentiodynamic polarization curves for Carbon steel in 1M HCL with different concentrations of SDS a) $1 \times 10^{-4}M$, b) $8 \times 10^{-4}M$, c) $1 \times 10^{-3}M$, d) $8 \times 10^{-3}M$, e) $4 \times 10^{-2}M$ at 20 °C, 30 °C, 40 °C and 50 °C

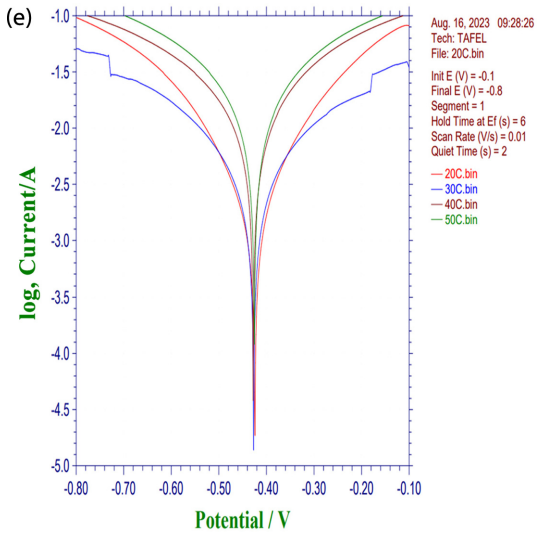

Fig. 2. Potentiodynamic polarization curves for Carbon steel in 1M HCL with different concentrations of SDS a) 1 × 10^{-4}*M*, b) 8 × 10^{-4}*M*, c) 1 × 10^{-3}*M*, d) 8 × 10^{-3}*M*, e) 4 × 10^{-2}*M* at 20 °C, 30 °C, 40 °C and 50 °C

oxidation curves gradually decreased. At SDS concentrations below the critical micelle concentration (CMC), the current is lower than the blank, and the peak potential shows minimal shift. However, when the inhibitor concentration exceeds the CMC (C> 8 × 10^{-3} M), a shift in the peak potential is observed. The corrosion current density was found to decrease as the inhibitor concentration increased, reaching a minimum at the CMC. Despite this, the inhibitor does not significantly impede the rates of cathodic reduction (hydrogen evolution) or anodic reactions (metal dissolution) occurring at the respective sites on the carbon steel surface in the HCl solution [14,15].

At 20 °C, carbon steel treated with a 1 × 10^{-4} M SDS inhibitor demonstrated a more positive corrosion potential (Ecorr = -0.4167 VSCE) compared to the untreated Carbon steel alloy (-0.4382 VSCE). As shown in Table 2, the corrosion current densities (Icorr) for carbon steel with the SDS inhibitor are lower than those of the untreated alloy. In particular, the sample treated with 4×10^{-2} M SDS inhibitor exhibited the lowest corrosion current density (Icorr = 1.600 mA/cm^2). Additionally, the inhibition efficiency (IE%) increases as the concentration of SDS inhibitor rises, reaching a maximum of 70% in the solution with 1.0 M HCl + 4 × 10^{-2} M SDS, suggesting enhanced surface coverage [16]. These findings indicate that the aqueous solutions containing 1 M HCl and varying concentrations of SDS inhibitor (ranging from 1 × 10^{-4} to 4 × 10^{-2} M) are effective in reducing the corrosion rates of the tested samples.

The study provides a comprehensive analysis of how temperature and SDS concentration influence the corrosion inhibition of carbon steel in an acidic medium, revealing a complex interplay between these variables and the underlying electrochemical processes. As temperature increases, the corrosion current density (i_{corr}) rises significantly, indicating an accelerated corrosion process due to enhanced kinetic energy of reacting species. However, SDS mitigates this effect, though its efficiency slightly decreases at higher temperatures, possibly due to the desorption of SDS molecules or partial breakdown of the protective film. This suggests that while SDS is effective, its performance may diminish at elevated temperatures, requiring higher concentrations or additional stabilizing agents. On the other hand, the concentration of SDS plays a crucial role in determining corrosion inhibition efficiency (EI%), with higher concentrations leading to greater protection. At the lowest concentration (1 × 10^{-4} M), inhibition efficiency is modest, but as concentration increases to 8 × 10^{-3} M and 4 × 10^{-2} M, efficiency rises significantly, reaching up to 70% at 20 °C. This increase is attributed to the increased surface coverage and tighter packing of SDS molecules, forming a more effective protective film. When considering both temperature and concentration, the data suggest that SDS provides substantial corrosion protection, particularly at lower temperatures where even lower concentrations can achieve high inhibition efficiencies. However, at higher temperatures, a higher SDS concentration is necessary to maintain similar protection levels, highlighting the temperature-dependent stability of the protective film. Overall, the study underscores the importance of selecting appropriate SDS concentrations based on specific operating conditions to optimize its efficacy as a corrosion inhibitor in acidic environments.

The SDS surfactant primarily acts as an inhibitor by adsorbing onto the steel surface, reducing both anodic and cathodic reactions without necessarily inducing passivation. The lack of a clear passive region in the anodic range might be due to the nature of the SDS as a surfactant, which does not strongly block anodic sites to the extent

Table 3. Thermodynamic activation parameters of carbon steel in 1 M HCl in the absence and presence of SDS

Inhibitor	Con.,(M)	$E_a\left(\frac{KJ}{mol}\right)$	$\Delta H\left(\frac{KJ}{mol}\right)$	$\Delta S\left(\frac{KJ}{mol}\right)$
HCl	0.0	43.9	44.4	-48.2
SDS	1×10^{-4}	47.6	45.11	-48.5
	8×10^{-4}	50.0	47.44	-41.01
	1×10^{-4}	52.0	49.49	-37.03
	8×10^{-4}	51.8	49.3	-38.09
	4×10^{-4}	56.8	54.29	-23.30

required for passivation but still effectively reduces the corrosion current density, as seen in our results. This inhibition is more likely due to a decrease in the effective area available for both anodic and cathodic reactions rather than the formation of a protective passive oxide layer, which is typically responsible for passivation.

The potentiodynamic polarization curves in our study show a decrease in the corrosion current density with increasing concentrations of SDS, indicating its efficacy as a corrosion inhibitor, though without the formation of a passive layer. This is consistent with the mechanism where SDS molecules adsorb on the steel surface, creating a barrier that limits the access of corrosive species rather than forming a passivating oxide layer.

4.2 Thermodynamic and activation parameters study

The understanding of the adsorption mechanism of inhibitor molecules on metal surfaces is heavily influenced by the thermodynamic parameters of adsorption. The impact of temperature on the adsorption of Carbon steel in the presence of SDS was investigated over a range of 20 ºC to 50 ºC, under both inhibited and uninhibited conditions. The inhibition mechanism was examined by comparing the activation energy (Ea) with and without the inhibitor. The activation energy was calculated using the Arrhenius equation, while the adsorption enthalpy (ΔH_{ads}) and adsorption entropy (ΔS_{ads}) were derived to further analyze the corrosion behavior of Carbon steel under these conditions. The relevant data are presented in Table 3 and plotted using the Arrhenius equation [17]. The data is given in below Table 3 and plotted using the following Arrhenius equation (7).

$$C_R = Ae^{-\frac{Ea}{RT}} \quad (7)$$

Where CR denotes the corrosion rate, R is the universal gas constant, T represents the absolute temperature, and

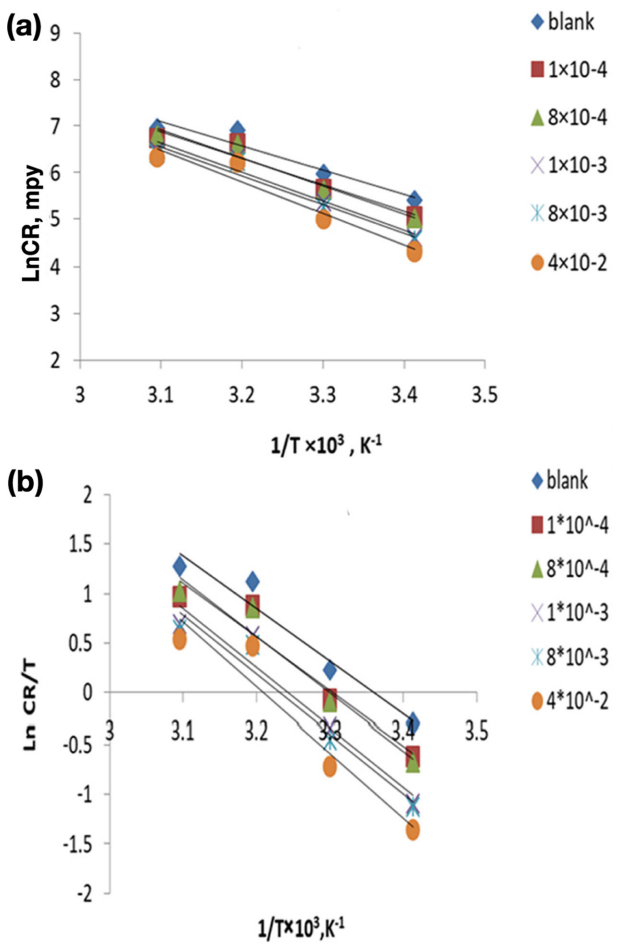

Fig. 3. (a) Arrhenius plot (b) transition plot obtained for the dissolution process of Carbon steel in 1.0 M HCl in the absence and presence of the SDS inhibitor

Table 4. Langmuir,Freudlich, and Temkin adsorption parameters of adsorption of the inhibitor SDS on the carbon steel surface at different temperatures

Temperture	K	ΔG^{o}_{ads}	*Slop*	R^2
Langmuir				
293 *K*	1250	-27154.8	1.4894	0.9969
303 *K*	909.09	-27279.3	1.5825	0.9925
313 *K*	1666.66	-29757.0	1.9837	0.9991
323 *K*	555.55	-27757.4	2.0442	0.9925
Freudlich				
293 *K*	1.2244	-10277.2	0.1519	0.7638
303 *K*	1.0902	-10335.4	0.152	0.8291
313 *K*	0.9380	-10285.4	0.1463	0.7346
323 *K*	0.9964	-10776.0	0.1917	0.5886
Temkin				
293 *K*	0.9380	-9628.22	0.0689	0.7798
303 *K*	0.9473	-9981.56	0.0642	0.8424
313 *K*	0.9632	-10354.2	0.0521	0.7489
323 *K*	0.9613	-10679.9	0.0572	0.6785

A stands for the pre-exponential factor. The Arrhenius plot, which is depicted, allows for the determination of the activation energy (Ea) values from its slope, both in the presence and absence of the inhibitor across different temperatures. These Ea values are crucial for understanding the mechanism of corrosion inhibition. Additionally, other activation parameters, such as the entropy (ΔS_{ads}) and enthalpy (ΔH_{ads}) of adsorption, were calculated for the corrosion process using the Van't Hoff equation, both with and without the inhibitor [18].

$$Ln\left[\frac{CR}{T}\right] = Ln\frac{R}{Nh} + \left[\frac{\Delta S}{R}\right] - \left[\frac{\Delta H}{RT}\right] \quad (8)$$

N represents Avogadro's number, h is Planck's constant, and R is the universal gas constant. The graphs of log (CR/T) versus 1/T were plotted, and from the slope (−ΔH/2.303R) and the intercept [log(R/Nh) + (ΔS/2.303R)] of these plots, the values of ΔH and ΔS were determined.

The thermodynamic parameters offer important insights into the effectiveness of corrosion inhibitors for carbon steel. Without any inhibitors, the initial activation energy is 43.9 kJ/mol, accompanied by an enthalpy of 44.4 kJ/mol and an entropy of -48.2 kJ/mol.

The surfactant SDS exhibits varying effectiveness as a corrosion inhibitor. At a concentration of 4×10^{-2} M, the activation energy reaches a maximum value of 56.8 kJ/mol, accompanied by an enthalpy of 54.29 kJ/mol. This further strengthens its potential in preventing corrosion.

While an entropy of -23.30 kJ/mol, highlighting the dynamic nature of its interaction with the metal surface.

4.3 Adsorption isotherms

Adsorption isotherms play a crucial role in comprehending the mechanism of corrosion inhibition, as they offer insights into the interaction between the adsorbed molecules and the metallic surfaces [3], the commonly utilized isotherms include Langmuir, Freundlich, and Temkin. The best appropriate was found with the Langmuir model, equaion (9) [15].

$$\frac{C}{\theta} = \frac{1}{K} - C \quad (9)$$

where θ is the degree of surface coverage, C is the inhibitor concentration and K is the equilibrium constant of adsorption. The value of θ for different concentrations of the inhibitor in 1.0 M HCl solution has been evaluated

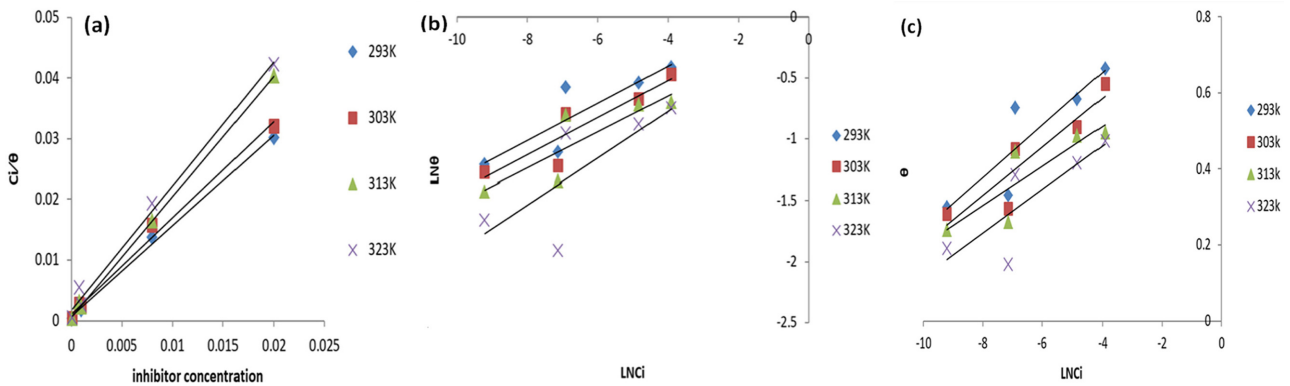

Fig. 4. Adsorption isotherm plots of (a) langmuir, (b) freudlich, (c) temkin of SDS on Carbon steel in 1 M HCl at different temperatures

from the gravimetric measurements.

Plots of C/θ against C at (20-50 ºC) are generated, Producing straight lines with the linear correlation of slope near unity indicates that the Langmuir adsorption isotherm governs the adsorption of SDS on the CS interface at all temperatures under investigation.

(R^2:0.9969, 0.9925, 0.9991 and 0.9925) at 293k, 303k, 313k and 323k, respectively. The surface coverage (θ) values were determined using equation (10) [19].

$$\theta = IE\%/100 \quad (10)$$

The adsorption constant (K_{ads}) values for SDS were determined by calculating the point where the straight lines intersected the x-axis in (Fig. 5). The standard free energy values (ΔG_{ads}) were computed using the equation (11) [20].

$$\Delta G_{ads} = -RTln(55.5K_{ads}) \quad (11)$$

4.4 Surface morphological study

Scanning electron microscopy (SEM) is essential for corrosion inhibition research as it offers a comprehensive analysis of surface morphology at the micro and nanoscale. It enables researchers to evaluate the changes in surface features, such as holes and fissures, by examining the material surface either before or after the application of corrosion inhibitors. SEM is also instrumental in the characterisation of corrosion products by determining their morphology and elemental composition, which is crucial for comprehending the corrosion process. Furthermore, SEM assists in the assessment of the distribution and integrity of the inhibitor deposit on the material surface, providing valuable information regarding the inhibition mechanisms. SEM is a critical instrument in corrosion research due to its ability to quantify surface defects such as pits and fractures, which provides essential data on the effectiveness of the corrosion inhibitor [21-23].

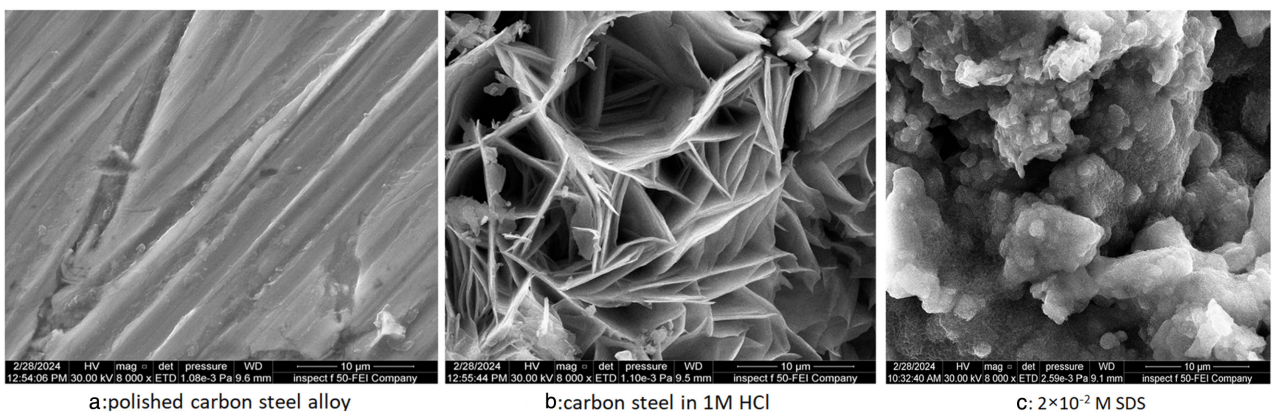

Fig. 5. Surface morphology for MS in 1.0 M HCl in the presence and absence of inhibitor

The polished carbon steel surface is depicted in the SEM image Fig. 5a The image illustrates a mechanically polished metal surface with parallel striations that is relatively smooth and uniform. The refining process, which is responsible for the removal of surface irregularities and the preparation of the metal for further analysis or treatment, is the cause of these striations. The carbon steel surface is currently free of corrosion damage, as evidenced by the absence of significant fissures, fractures, or irregularities.

In the SEM image Fig. 5b, which depicts carbon steel that has been exposed to 1M hydrochloric acid (HCl), the surface morphology has undergone a significant transformation in comparison to the polished sample. The surface is characterised by deep fissures and irregular structures, which are indicative of severe corrosion. This is a common occurrence in acid attacks on carbon steel, where the dissolution of the iron matrix is facilitated by the aggressive chloride ions in HCl, resulting in the formation of corrosion products and extensive pitting. The image implies that the carbon steel is highly susceptible to corrosion in acidic environments in the absence of any inhibitor.

The SEM image Fig. 5c represents the carbon steel surface after exposure to 2×10^{-2} M SDS in HCl. The surface appears significantly different from that in image B. The presence of SDS has led to the formation of a protective layer on the carbon steel, which is evident from the granular and somewhat compact structure visible in the SEM image. This layer likely consists of adsorbed SDS molecules that form a barrier, reducing the direct contact between the steel surface and the acidic environment, thereby inhibiting corrosion. The reduced roughness and fewer pits suggest that SDS acts effectively as a corrosion inhibitor under these conditions, reducing the severity of the acid attack compared to the untreated sample in Fig. 5b [24-26].

Atomic Force Microscopy (AFM) plays a crucial role in the study of corrosion inhibition by providing detailed topographical images and surface property measurements at the nanoscale. This technique allows researchers to observe the surface morphology of materials before and after the application of corrosion inhibitors, offering insights into the effectiveness of these inhibitors in real-time. By analyzing surface roughness, adhesion forces, and other surface interactions, AFM helps in understanding the mechanisms by which corrosion inhibitors protect metals, aiding in the development of more efficient and targeted corrosion prevention strategies [27]. The AFM analysis of the 2D and 3D descriptions provides a detailed conception of the carbon steel surface before and after exposure to 1 M HCl, both in the absence and presence of the inhibitors, captured at room temperature over a range of (0-50 μm). The pictures were used to quantify the average surface roughness, revealing significant insights into the protective efficacy of the inhibitors [28-30]. (Fig. 6a) indicates that the polished surface of the carbon steel electrode is rather soft and exhibits a consistent pattern. The average roughness value (Ra) is around 98.7 nm and after the electrode has been immersed in 1 M HCl in the absence of SDS,shown in Fig. 6b, Cracks form in addition to the uneven surface (Ra increases to 382 nm) due to the acid's corrosive effect on the carbon steel.

When the SDS are present (Fig. 6c), the average roughness value is 131.5 nm. with a more polished and even texture. It is hypothesized that this impact of inhibition occurs as a consequence of the decrease in corrosion-related harm caused by the creation of a defensive coating on the surface of carbon steel,thus reducing the interaction between the steel and the highly corrosive acidic solution.

4.5 Quantum chemical study

In order to gain a more comprehensive comprehension of electrical structure and to make comparisons with the experimental inhibition efficacy of the inhibitors under investigation, PM3 was performed, The calculated parameters such as energy of the highest occupied molecular orbital (E_{HOMO}), energy of the lowest unoccupied molecular orbital (E_{LUMO}), Energy gap (Eg), Ionization potential (I), electron affinity (A), chemical hardness (η), chemical softness (ζ), electronegativity (X), chemical potential (μ), global index (ω), (ΔN), ($\Delta\Psi$), ($E_{b\text{-}d}$) were calculated and summarized in Table 5 (Fig. 7).

The quantum PM3 analysis of Sodium Dodecyl Sulfate (SDS) as a corrosion inhibitor for carbon steel in hydrochloric acid reveals key insights into its electronic properties and reactivity. The HOMO energy of -13.432 eV suggests that SDS is less likely to donate electrons,

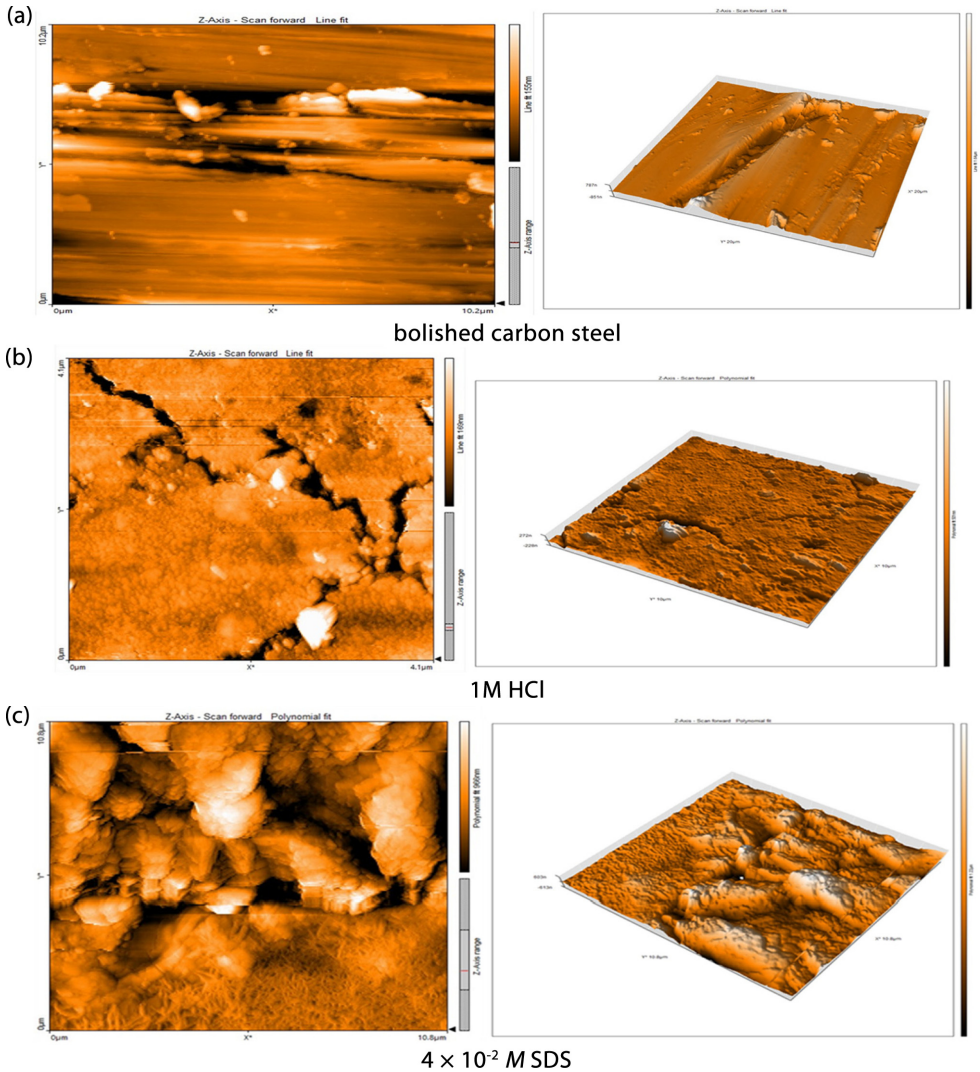

Fig. 6. AFM (3D) and (2D) images of the metal surface in different situations

Table 5. Calculated quantum chemical parameters for SDS

Inhibitor	SDS
Compute properties	
HOMO	-13.432
LUMO	1.203
Energy gap Eg	14.635
Ionization potential I	13.432
electron affinity A	-1.203
chemical hardness η	7.3175
chemical softness ζ	0.0683
electronegativity X	6.1145
chemical potential μ	-6.1145
global index ω	2.5546
NΔ	0.0605
ΨΔ	0.0302
Eb-d	-1.8293

while the LUMO energy of 1.203 eV indicates a moderate capacity to accept electrons. The large energy gap of 14.635 eV between HOMO and LUMO suggests that SDS is chemically stable, which may contribute to its effectiveness as an inhibitor. The ionization potential, equal to the HOMO energy, confirms SDS's stability and resistance to ionization. However, the negative electron affinity of -1.203 eV indicates a limited tendency to gain electrons. SDS exhibits high chemical hardness (7.3175 eV) and low softness (0.0683 eV), suggesting that it is inert and resistant to changes in its electron cloud, reinforcing its stability. The moderate electronegativity (6.1145 eV) and negative chemical potential (-6.1145 eV) reflect SDS's balanced tendency to attract electrons, though it is not overly reactive. The global electrophilicity index (2.5546 eV) indicates SDS is not a strong electrophile, and the low nucleophilic (0.0605) and electrophilic

Inhibitor	HOMO	LUMO	Molecular Structure
SDS	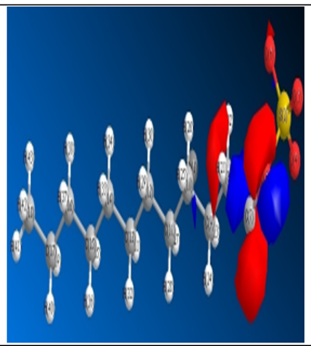	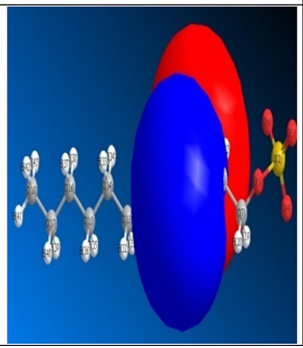	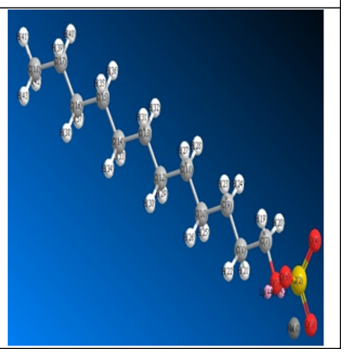

Fig. 7. Frontier molecule orbital density distributions of SDS

(0.0302) indices suggest limited reactivity in donating or accepting electrons. Lastly, the negative back-donation energy (-1.8293 eV) implies that SDS has a limited ability to donate electrons back to the metal surface after adsorption, suggesting that its inhibition mechanism might involve physical adsorption or forming a protective barrier rather than strong chemical interactions with the steel. Overall, the analysis suggests that SDS is a stable and moderately reactive inhibitor, likely effective in forming a protective layer on carbon steel in hydrochloric acid, though it may not strongly interact with the metal through electron exchange.

4.6 Mechanism of SDS as corrosion inhibitor

The mechanism of Sodium Dodecyl Sulfate (SDS) as a corrosion inhibitor for carbon steel in hydrochloric acid involves a combination of physical adsorption and the formation of a protective barrier on the steel surface. SDS dissociates in the acidic environment, and the negatively charged sulfate head groups adsorb onto the positively charged areas of the steel, aided by electrostatic attraction and van der Waals interactions between the alkyl chains and the steel surface. This adsorption leads to the formation of a protective layer that acts as a physical barrier, reducing the steel's direct exposure to the corrosive environment and limiting the access of aggressive species like H^+ and Cl^- ions. The hydrophobic nature of the alkyl chains further repels water, enhancing the protective effect. However, the theoretical analysis, showing a large HOMO-LUMO gap and low chemical softness, suggests that SDS does not strongly participate in electron transfer processes with the steel surface, indicating that the inhibition is mainly due to physical adsorption rather than chemical interaction. This helps explain why the efficiency is about 70% rather than higher, as the protective layer might not completely cover the steel surface, leaving some areas exposed to corrosion. Additionally, competitive adsorption with chloride ions and the dynamic nature of SDS adsorption and desorption on the steel surface further contribute to the partial inhibition efficiency observed experimentally.

5. Conclusions

1. Potentiodynamic polarization revealed that SDS achieved a 70.0% inhibition efficiency, indicating significant protection. SEM analysis confirmed a homogeneous corrosion layer on the steel surface, though localized corrosion penetration was also observed.

2. The adsorption of SDS molecules onto the carbon steel surface followed the Langmuir adsorption isotherm, indicating a monolayer adsorption process with uniform surface coverage.

3. Computational studies highlighted the critical role of SDS's electronic properties in its corrosion inhibition efficiency. The large HOMO-LUMO gap and high chemical hardness suggest that SDS inhibits corrosion primarily through physical adsorption rather than strong chemical interactions.

These findings not only show that SDS may effectively suppress corrosion of carbon steel in acidic settings but also point to potential optimization targets for localized corrosion.

References

1. A.Yousefi, S. Javadian, and J. Neshati, A new approach to study the synergisticinhibition effect of cationic and anionic surfactants on the corrosion of mild steel in HCl solution, *Industrial & Engineering Chemistry Research*, **53**, 5475 (2014). Doi: https://doi.org/10.1021/ie402547m
2. S.Javadian, A. Yousefi, and J. Neshati, Synergistic effect of mixed cationic and anionic surfactants on the corrosion inhibitor behavior of mild steel in 3.5% NaCl, *Applied Surface Science*, **285**, 674 (2013). Doi: https://doi.org/10.1016/j.apsusc.2013.08.109
3. M. Mobin, S. Zehra, and M. Parveen, L-Cysteine as corrosion inhibitor for mild steel in 1 M HCl and synergistic effect of anionic, cationic and non-ionic surfactants.*Journal of Molecular Liquids*, **216**, 598 (2016). Doi: https://doi.org/10.1016/j.molliq.2016.01.087
4. K. R. Ansari, , M. A. Quraishi, and A. Singh, Schiff's base of pyridyl substituted triazoles as new and effective corrosion inhibitors for mild steel in hydrochloric acid solution,*Corrosion Science*, **79**, 5 (2014). Doi: https://doi.org/10.1016/j.corsci.2013.10.009
5. A. Ehsani, H. Mohmmad Shiri, M. G. Mahjani, R. Moshrefi, M. Hadi, and N. Soltanpour, Theoretical, common electrochemical and electrochemical noise investigation of inhibitory effect of new organic compound nanoparticles in the corrosion of stainless steel in acidic solution*Transactions of the Indian Institute of Metals*, **69**, 1519 (2016). Doi: https://doi.org/10.1007/s12666-015-0724-4
6. D. K. Singh, S. Kumar, G. Udayabhanu, and Rohith P. John, 4 (N, N-dimethylamino) benzaldehyde nicotinic hydrazone as corrosion inhibitor for mild steel in 1 M HCl solution: An experimental and theoretical study, *Journal of molecular liquids*, **216**, 738 (2016). Doi: https://doi.org/10.1016/j.molliq.2016.02.012
7. R. Guo, T. Liu, and X. Wei, Effects of SDS and some alcohols on the inhibition efficiency of corrosion for nickel, *Colloids and Surfaces A: Physicochemical and Engineering Aspects*, **209**, 37 (2002). Doi: https://doi.org/10.1016/S0927-7757(02)00032-8
8. M. F. Heragh, and H. Tavakoli, Synergetic effect of the combination of Prosopis Farcta extract with sodium dodecyl sulfate on corrosion inhibition of St37 steel in 1M HCl medium, *Journal of Molecular Structure*, **1245**, 131086 (2021). Doi: https://doi.org/10.1016/j.molstruc.2021.131086
9. F.E-T.Heakal, M. A. Deyab, M. M. Osman, M. I. Nessim, and A. E. Elkholy, Synthesis and assessment of new cationic gemini surfactants as inhibitors for carbon steel corrosion in oilfield water, *RSC advances*, **7**, 47335 (2017). Doi: https://doi.org/10.1039/C7RA07176K
10. M. A. Erteeb, E. E. Ali-Shattle, S. M. Khalil, H. A. Berbash, Z. E. Elshawi, Computational studies (DFT) and PM3 theories on thiophene oligomers as corrosion inhibitors for iron, *American Journal of Chemistry*, **11**, 1 (2021). Doi: https://doi.org/10.5923/j.chemistry.20211101.01
11. O. A. A. El-Shamy, Semiempirical Theoretical Studies of 1, 3-Benzodioxole Derivatives as Corrosion Inhibitors, *International Journal of Corrosion*, **1**, 8915967 (2017). Doi: https://doi.org/10.1155/2017/8915967
12. A. H. Radhi, AB. Ennas, F. A. Khazaal, Z. M. Abbas, O. H. Aljelawi, S. D. Hamadan, H. A. Almashhadani, M. M. Kadhim, HOMO-LUMO energies and geometrical structures effecton corrosion inhibition for organic compounds predict by DFT and PM3 methods, *NeuroQuantology*, **18**, 37 (2020). Doi: http://doi.org/10.14704/nq.2020.18.1.NQ20105
13. H. M. Abd El-Lateef, M.A. Abo-Riya, and A.H. Tantawy, Empirical and quantum chemical studies on the corrosion inhibition performance of some novel synthesized cationic gemini surfactants on carbon steel pipelines in acid pickling processes, *Corrosion Science*, **108**, 94 (2016). Doi: https://doi.org/10.1016/j.corsci.2016.03.004
14. R. Fuchs-Godec, and V. Doleček, A effect of sodium dodecylsulfate on the corrosion of copper in sulphuric acid media, *Colloids and Surfaces A: Physicochemical and Engineering Aspects*, **244**, 73 (2004). Doi: https://doi.org/10.1016/j.colsurfa.2004.05.015
15. P. Roy, and D. Sukul, Protein–surfactant aggregate as a potential corrosion inhibitor for mild steel in sulphuric acid: zein–SDS system, *RSC Advances*, **5**, 1359 (2015). Doi: https://doi.org/10.1039/C4RA12821D
16. H. Song, Z. Xu, L. Benabou, Z. Yin, H. Guan, H. Yan, L. Choo, Z. Hu, and X. Wang, Sodium dodecyl sulfate (SDS) as an effective corrosion inhibitor for Mg-8Li-3Al alloy in aqueous NaCl: A combined experimental and theoretical investigation, *Journal of Magnesium and Alloys*, **11**, 287 (2023). Doi: https://doi.org/10.1016/j.jma.2021.07.006
17. R. Murthy, K. R. Krishna, and C. N. Sundaresan, Exploring the role of Sodium dodecyl sulphate in presence of 2-thioureidobenzoxazole as enhancer of corrosion inhibition of mild steel in 2M HCl solution, *International Jour-*

nal of Electrochemical Science, **17**, 22094 (2022). Doi: https://doi.org/10.20964/2022.09.43

18. N. Saini, R. Kumar, H. Lgaz, R. Salghi, I.-M. Chung, S. Kumar, S. Lata, Minified dose of urispas drug as better corrosion constraint for soft steel in sulphuric acid solution, *Journal of Molecular Liquids*, **269**, 371 (2018). Doi: https://doi.org/10.1016/j.molliq.2018.08.070
19. M. A. Albo Hay Allah, Asim A. Balakit, H. I. Salman, A. A. Abdulridha, and Y. Sert, New heterocyclic compound as carbon steel corrosion inhibitor in 1 M H2SO4, high efficiency at low concentration: experimental and theoretical studies,*Journal of Adhesion Science and Technology*, **37**, 525 (2023). Doi: https://doi.org/10.1080/01694243.2022.2034588
20. A. A. Abdulridha, M. A. A. H. Allah, S. Q. Makki, Y. Sert, H. E. Salman, and A. A. Balakit, Corrosion inhibition of carbon steel in 1 M H_2SO_4 using new Azo Schiff compound: Electrochemical, gravimetric, adsorption, surface and DFT studies, *Journal of Molecular Liquids*, **315**, 113690 (2020). Doi: https://doi.org/10.1016/j.molliq.2020.113690
21. C.Verma, E. E. Ebenso, I. Bahadur, M. A. Quraishi, An overview on plant extracts as environmental sustainable and green corrosion inhibitors for metals and alloys in aggressive corrosive media, *Journal of molecular liquids*, **266**, 577 (2018). Doi: https://doi.org/10.1016/j.molliq.2018.06.110
22. V. S. Saji, and J. Thomas, Nanomaterials for corrosion control, *Current Science*, **92**, 51 (2007). Doi: https://www.jstor.org/stable/24096821
23. S. Baumeister, Replacing short-haul flights with land-based transportation modes to reduce greenhouse gas emissions: The case of Finland, *Journal of Cleaner Production*, **225**, 262 (2019). Doi: https://doi.org/10.1016/j.jclepro.2019.03.329
24. S. A. Umoren, M. M. Solomon, I. B. Obot, R. K. Suleiman, A critical review on the recent studies on plant biomaterials as corrosion inhibitors for industrial metals, *Journal of Industrial and Engineering Chemistry*, **76**, 91 (2019). Doi: https://doi.org/10.1016/j.jiec.2019.03.057
25. Y. El Kacimi, H. El Bakri, K. Alaoui, R. Touir, M. Galai, M. Ebn Touhami, M. Doubi, Synergistic effect study of Cetyl Trimethyl Ammonium Bromide with iodide ions at low concentration for mild steel corrosion in 5.0 M HCl medium, *Chemical Data Collections*, **30**, 100558 (2020). Doi: https://doi.org/10.1016/j.cdc.2020.100558
26. M. Goyal, H. Vashisht, A. Kumar, S. Kumar, I. Bahadur, F. Benhiba, A. Zarrouk, Isopentyltriphenylphosphonium bromideionic liquid as a newly effective corrosion inhibitor on metal-electrolyte interface in acidic medium: Experimental, surface morphological (SEM-EDX & AFM) and computational analysis, *Journal of Molecular Liquids*, **316**, 113838 (2020). Doi: https://doi.org/10.1016/j.molliq.2020.113838
27. F. Mansfeld, Electrochemical impedance spectroscopy (EIS) as a new tool for investigating methods of corrosion protection, *Electrochimica Acta*, **35**, 1533 (1990). Doi: https://doi.org/10.1016/0013-4686(90)80007-B
28. A. S. El-Tabei, O. E. El-Azabawy, N. M. El Basiony, M. A. Hegazy, Newly synthesized quaternary ammonium bis-cationic surfactant utilized for mitigation of carbon steel acidic corrosion; theoretical and experimental investigations, *Journal of Molecular Structure*, **1262**, 133063 (2022).Doi: https://doi.org/10.1016/j.molstruc.2022.133063
29. S. Jayakumar, T. Nandakumar, M. Vadivel, C. Thinaharan, R. P. George, and J. Philip, Corrosion inhibition of mild steel in 1 M HCl using Tamarindusindica extract: electrochemical, surface and spectroscopic studies, *Journal of Adhesion Science and Technology*, **34**, 713 (2020). Doi: https://doi.org/10.1080/01694243.2019.1681156
30. A. G. F. Shoair, M. M. Motawea, A. S. A. Almalki, M. M. A. H. Shanab, A. El-Basiony, H. A. Nasef, Expired terazosin as environmentally safe corrosion inhibitor for 1018 carbon steel in 1 M HCl solution: Experimental and computational studies, *International Journal of Electrochemical Science*, **19**, 100397 (2024).Doi: https://doi.org/10.1016/j.ijoes.2023.100397